

Short Communication

## Effect of Spin-Coating Cycle on the Properties of TiO<sub>2</sub> Thin Film and Performance of DSSC

S. N. Sadikin, M. Y. A. Rahman\*, A. A. Umar, M. M. Salleh

Institute of Microengineering and Nanoelectronics (IMEN), Universiti Kebangsaan Malaysia, 43600, Bangi, Selangor, Malaysia

\*E-mail: [mohd.yusri@ukm.edu.my](mailto:mohd.yusri@ukm.edu.my)

Received: 5 February 2017 / Accepted: 18 April 2017 / Published: 12 May 2017

---

TiO<sub>2</sub> thin films based dye-sensitized solar cell (DSSC) were prepared by sol-gel spin-coating method. The number of spin-coating was varied, 1, 2, 3, 5 and 7 times to get various thicknesses of TiO<sub>2</sub> thin film on the ITO substrate. The phase structure of anatase exists in all samples at the diffraction angle of 25.36° corresponding with the crystal plane (101). From FESEM observation, the morphological shape of all samples is agglomerate nanoparticle. The sample with higher number of spin coating has pores with its size becomes bigger at the highest spin coating number. The thickness of TiO<sub>2</sub> film increases with the increase of spin coating number. The absorption window increases with the spin coating number. The DSSC with 7 times spin coating number demonstrates the best power conversion efficiency ( $\eta$ ) which is 0.70% due to the broadest absorption window and lowest  $R_b$  and  $R_{ct}$ .

---

**Keywords:** DSSC, sol-gel, spin-coating, TiO<sub>2</sub>

### 1. INTRODUCTION

Dye-sensitized solar cells (DSSC) are the third generation of photovoltaic solar cell which converts visible light into electricity. Researches on DSSCs are being carried out worldwide because it is a low-cost solar cell with considerably high light to energy conversion efficiency [1]. The DSSC system is based on many metal oxide semiconductor materials such as TiO<sub>2</sub>, ZnO, SnO and many more. TiO<sub>2</sub> is widely used as photoanode because it is inexpensive, chemically stable due to its wide band gap, environmental friendly because it is non-toxic and high porosity hence allowing dye anchoring on the surface of TiO<sub>2</sub> reported by Sedghi et al. 2015 [2]. This leads to better light absorption in DSSC with TiO<sub>2</sub> film as the photoanode.

Many researches have been carried out to improve the performance of DSSC including studying the effect of TiO<sub>2</sub> thickness on the properties and performance of DSSC. These studies have been carried out by synthesizing the samples using various methods. For example, Zhang et al. 2014 studied the effect of TiO<sub>2</sub> film thickness on photovoltaic properties of DSSC [3]. In this study, the samples were prepared by using screen printing method and thickness of the TiO<sub>2</sub> films were varied by varying the number of printing layers. The performance of the device increased with the increase in printing layers. A study by Baglio et al. 2011 shows that DSSC with thicker layer of TiO<sub>2</sub> that is 10 μm gave the best performance because of better absorption of light, reduction of the recombination process and lower charge transfer resistance [4].

Various approaches have been employed in synthesizing TiO<sub>2</sub> such as hydrothermal method [5], solvothermal method [6], sol-gel method [7], direct oxidation method [8], chemical vapor deposition [9] and electrodeposition method [10]. Different synthesis method of TiO<sub>2</sub> can yield various morphologies such as nanotubes, nanowires, nanorods, and mesoporous structures as reported by Byranvand et al. 2013 in his review on the synthesis of nano-TiO<sub>2</sub> by using different methods [11]. Although sol-gel method is more simple and economical than other methods, it can produce TiO<sub>2</sub> nanoparticles with numerous morphologies such as sheets, tubes, particles, wires, rods, mesoporous and aerogels as stated by Sharma et al. 2014. In this work, TiO<sub>2</sub> was prepared by sol-gel method and was deposited on ITO glass substrates by spin-coating technique. The goal and originality of this work is to investigate the influence of spin coating number on the properties of TiO<sub>2</sub> thin films and performance of the DSSC.

## 2. EXPERIMENTAL

### 2.1 Preparation of TiO<sub>2</sub> thin films

The materials used in preparing TiO<sub>2</sub> films are titanium (IV) isopropoxide (97.0%), acetic acid (99.7%) purchased from Sigma-Aldrich and absolute ethanol (99.98%). TiO<sub>2</sub> solution was prepared by adding 1.80 ml of titanium (IV) isopropoxide which acts as precursor into 9.80 ml of ethanol which acts as solvent. While, the solution was being stirred, 0.3 ml of acetic acid was added into the solution. The mixture was stirred for about five hours. TiO<sub>2</sub> thin film was prepared by spin-coating method in which the TiO<sub>2</sub> solution was dropped onto ITO substrate and rotated at 2500 rpm for about 45 seconds. Then, the TiO<sub>2</sub> thin film was dried at 100 °C for 10 minutes. The number of spin-coating was varied for each sample to get various thicknesses of TiO<sub>2</sub> deposited on the ITO substrates with repeated process of drying in between the spin-coating technique. Five samples of TiO<sub>2</sub> thin films were prepared with different number of spin-coating which are 1, 2, 3, 5 and 7 times of spin-coating respectively. Finally, the TiO<sub>2</sub> thin films were annealed at 400 °C for 2 hours.

## 2.2 TiO<sub>2</sub> thin films characterization

The prepared samples were characterized by using X-ray diffractometer model Bruker D8 Advanced to study the elements and phase present in the samples. The diffraction angle,  $2\theta$  used was from  $10^\circ$  to  $80^\circ$ . The surface morphology examined from top view as well as the cross-section images were characterized by using a field emission electron microscope (FESEM) model MERLIN. This characterization was to compare the surface morphologies and thickness of TiO<sub>2</sub> layers on the substrates as the number of spin-coating was varied. The UV-Vis spectrophotometer was used to study the optical absorption of the samples.

## 2.3 Dye-sensitized solar cell (DSSC) fabrication and performance studies

An appropriate amount of N719 dye was dissolved in ethanol to get a solution with 0.5 mM concentration. Then, the TiO<sub>2</sub> samples were fully immersed in the dye solution and left for 15 hours. After 15 hours, a DSSC device was fabricated with TiO<sub>2</sub> film as the anode and platinum coated ITO obtained by sputtering technique as the counter electrode. An electrolyte containing iodide/triiodide redox couple was injected into the active area at the interface of TiO<sub>2</sub>/N719 and platinum counter electrode. The structure of the DSSC is shown in Fig. 1.

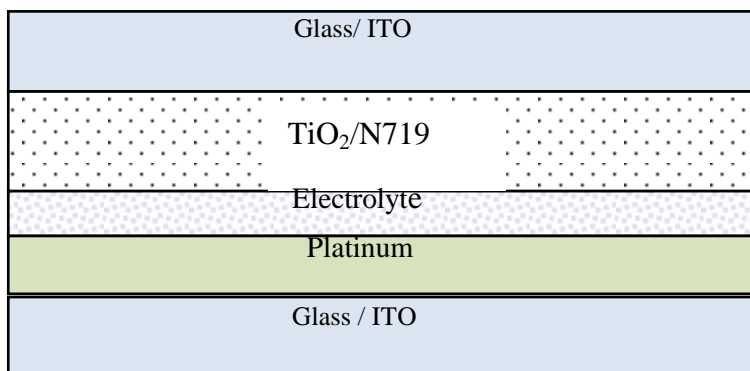


**Figure 1.** Structure of the DSSC

The  $J$ - $V$  characteristics of the device were obtained by examining it in the dark and under the light illumination of  $100 \text{ mW cm}^{-2}$ . The electrochemical impedance spectroscopy (EIS) analysis was also carried out to study the charge transport properties of the device as the thickness of the TiO<sub>2</sub> films was varied.

## 3. RESULTS AND DISCUSSION

The XRD spectra for TiO<sub>2</sub> thin films with different number of spin-coating are shown in Fig. 2. There are 4 peaks at the diffraction angle of  $25.36^\circ$ ,  $38.03^\circ$ ,  $48.14^\circ$  and  $54.96^\circ$  corresponding with (101), (004), (200) and (211) planes, respectively. The phase structure of the sample is anatase with

tetragonal crystal structure and is dominant at plane (101) for all samples. These results agree well with that reported by Jiménez González et al. 2007 who prepared TiO<sub>2</sub> films via sol-gel technique [12]. It is also found that the peak intensity at (101) plane slightly increases with the number of spin coating. The diffraction peaks of ITO substrate do not exist in these XRD patterns as the x-ray cannot penetrate the ITO since the thickness of TiO<sub>2</sub> film for each sample is high.

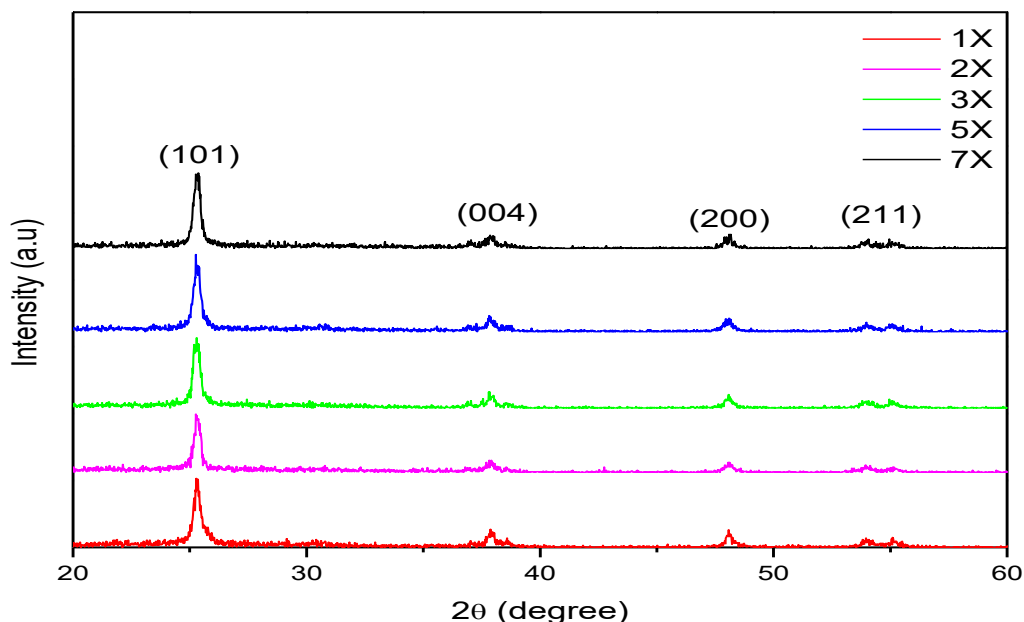
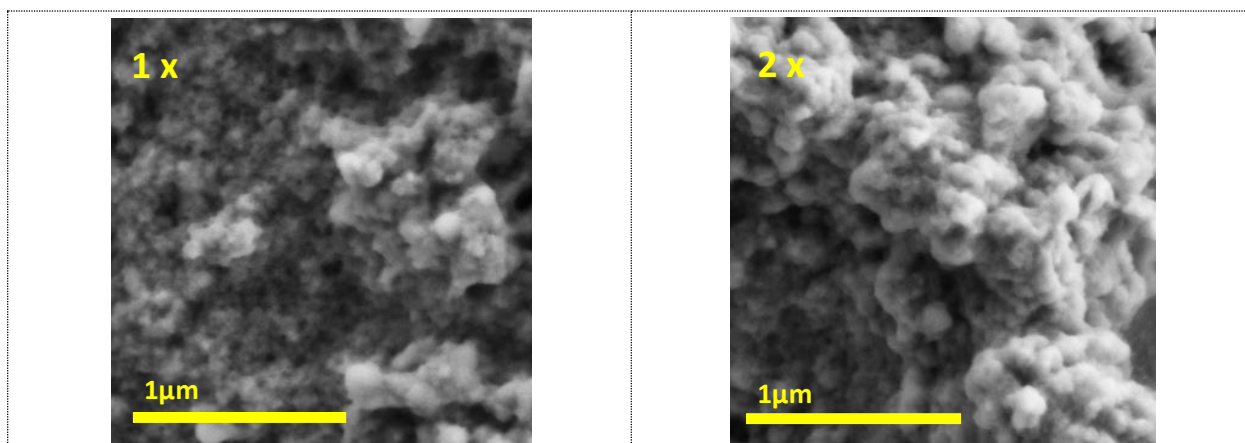
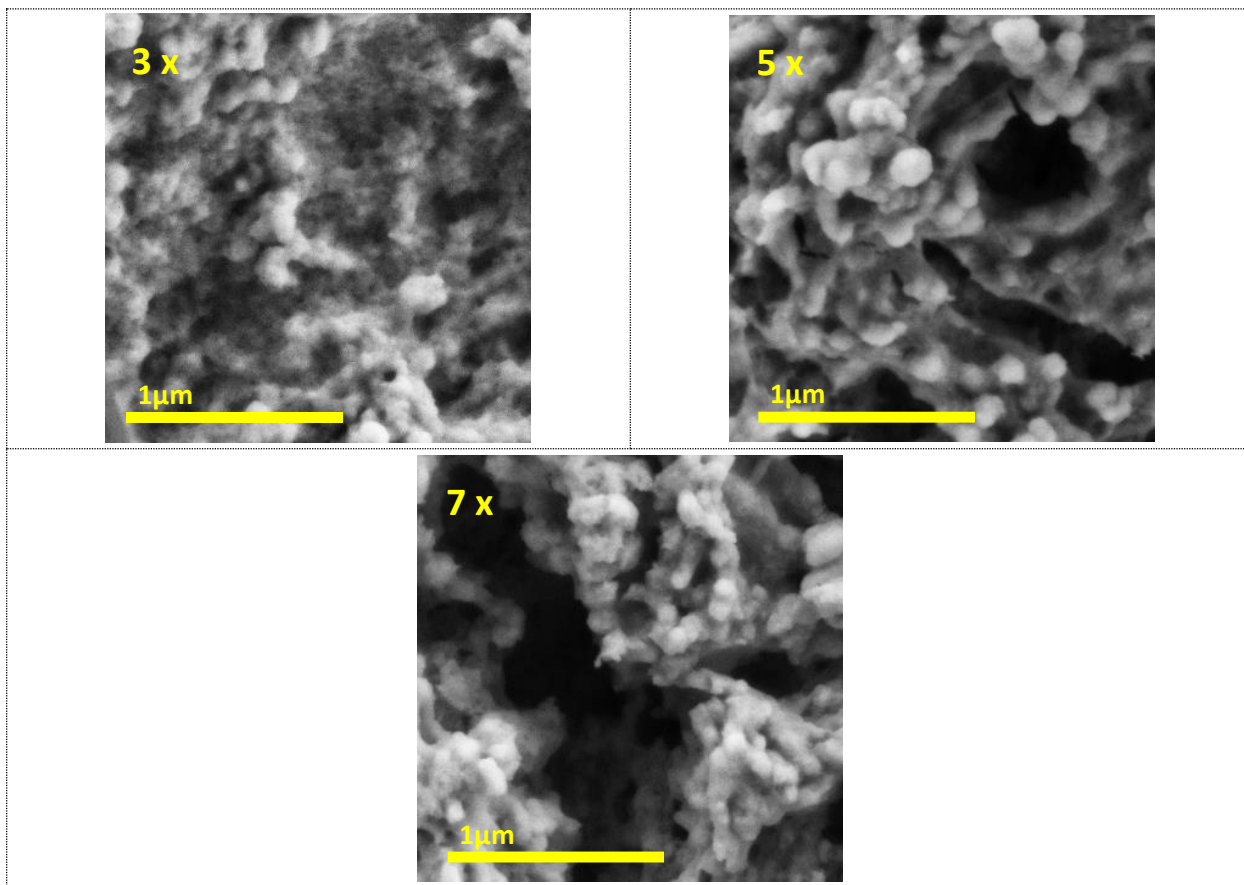


Figure 2. XRD spectra for TiO<sub>2</sub> thin films with different number of spin-coating

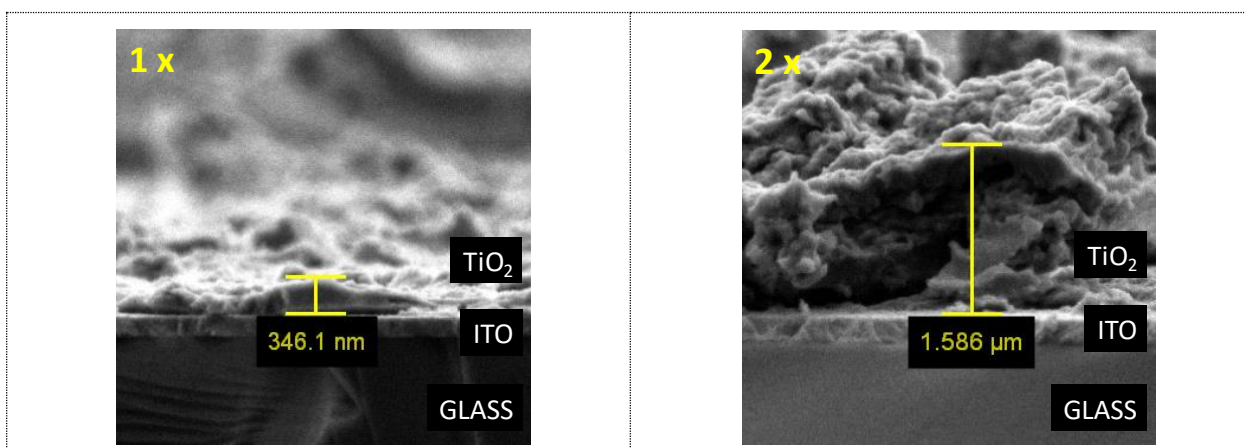
Fig. 3 shows the FESEM images of TiO<sub>2</sub> films with various spin coating cycles. From Fig. 3 (a), the sample with 1 cycle spin coating shows the TiO<sub>2</sub> nanoparticles are highly agglomerated with low porosity. As the spin coating number was increased to 2 times, the agglomerate size becomes bigger.

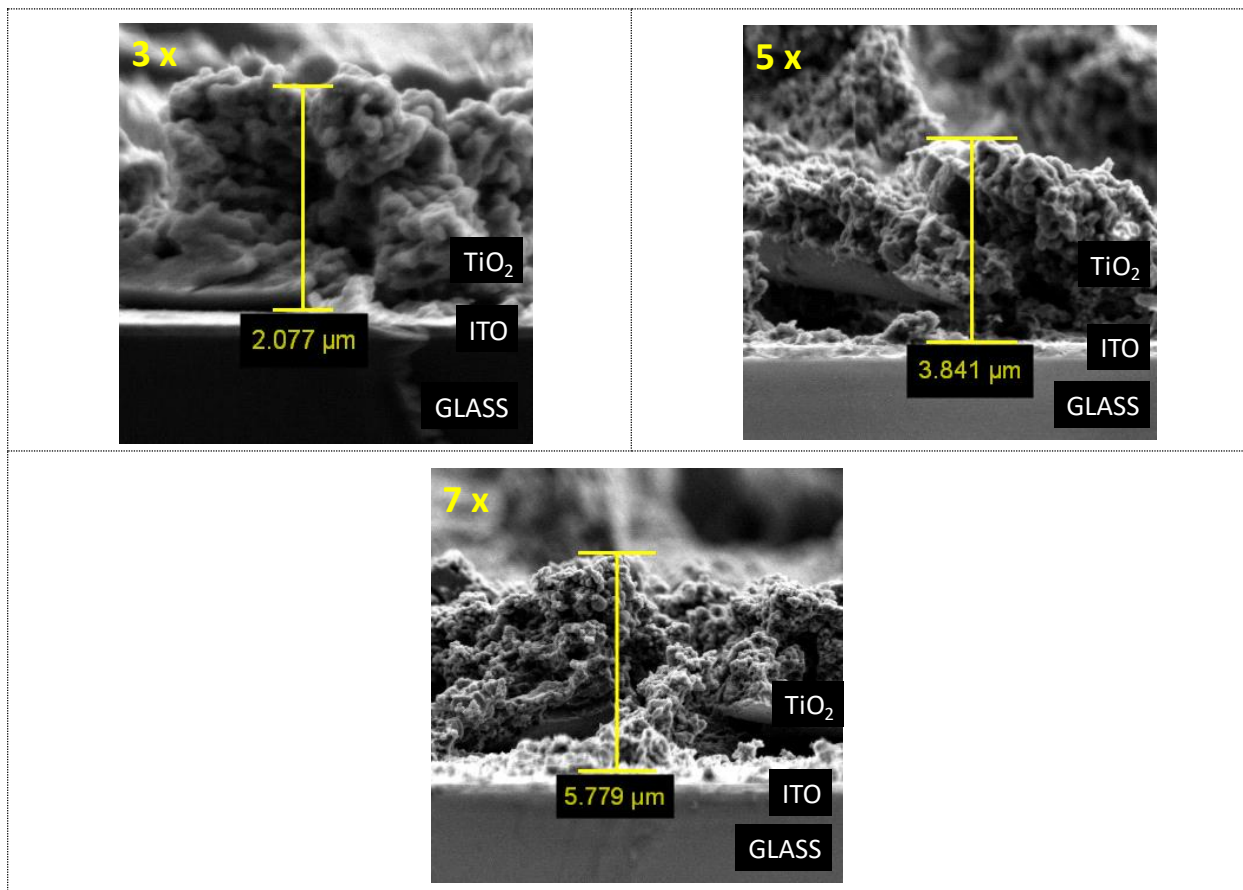




**Figure 3.** Top view FESEM images of TiO<sub>2</sub> thin films with different number of spin-coating

Once it was increased to 3 times, the small pores started to appear as shown in Fig. 3 (c). However, as the number of spin-coating increased to 5 times, the pore size becomes bigger as shown in Fig. 3(d). Finally, once the spin coating number was further increased to 7 times, the pore size becomes bigger than that of 5 times spin coating. The morphology of all samples is agglomerate nanoparticles.





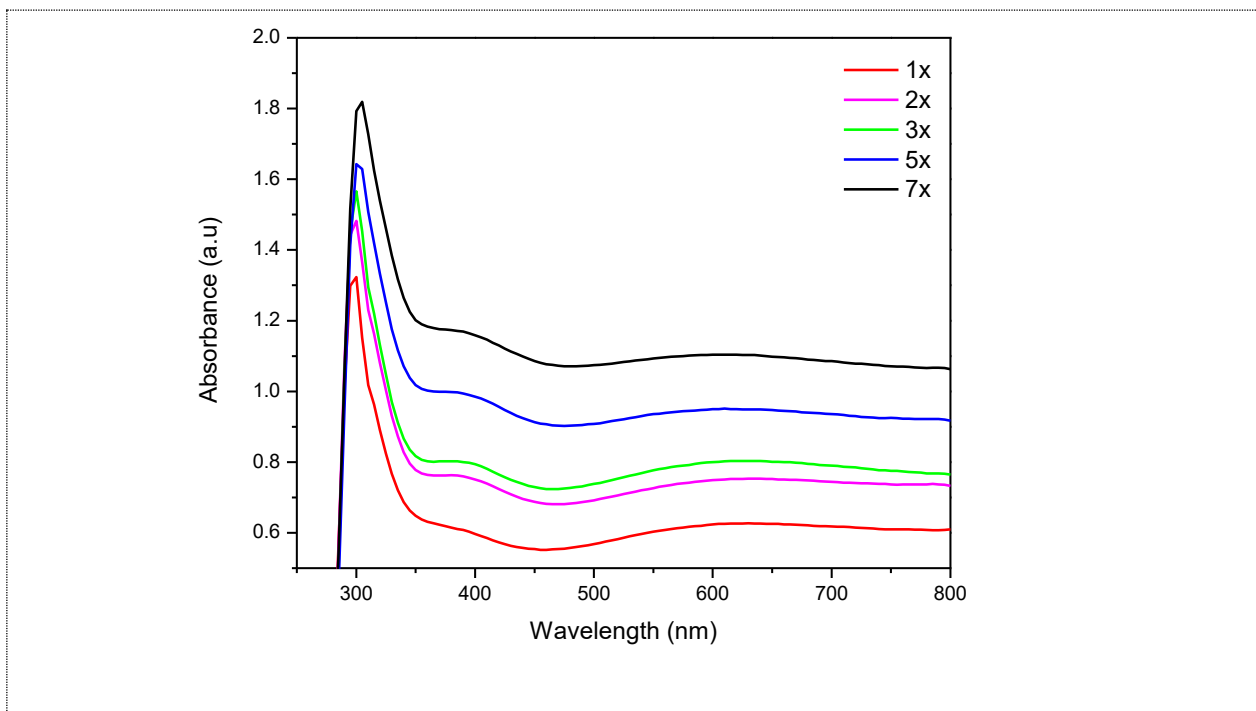
**Figure 4.** Cross-section images of TiO<sub>2</sub> thin films with different number of spin-coating

Fig. 4 displays the cross-sectional view of FESEM images for all samples. From the figure, the thickness of TiO<sub>2</sub> layer increases as the number of spin-coating increases. The thickness obtained for 1, 2, 3, 5 and 7 times of spin-coating are 346, 1586, 2077, 3841 and 5779 nm, respectively and listed in Table 1.

The UV-vis spectra for TiO<sub>2</sub> thin films with various number of spin-coating are shown in Fig. 5. The figure shows all samples absorb more light in ultra-violet (UV) region (300-340 nm). It is found that the light absorption in visible region is smaller than that in UV region for all samples. The intensity of absorption peak 300 nm increases with the spin coating number. The absorption window also increases with the increase in spin coating number. The absorption is higher when the thickness of TiO<sub>2</sub> thin film is increased. This allows higher amount of dye adsorption on the surface of the TiO<sub>2</sub> layer as indicated by Zhang et al. 2014 [3].

Fig. 6 shows the dark current curves for all devices utilizing the samples prepared with various spin coating cycles. From the figure, it is noticed that all devices do not show rectification property since the dark current in forward bias is slightly higher than that in reverse bias. Solar cell is said to behave like diode that exhibits like rectifier if it allows high current in forward bias with very small current in reverse bias. Also, from the figure, the device utilizing the sample with 7<sup>th</sup> cycles of spin coating possesses the highest forward current, while that utilizing 1<sup>st</sup> cycle of coating demonstrates the lowest current. In other words, the forward current increases with the number of spin coating. For the

negative bias current or so-called leak current, the device utilizing the 5<sup>th</sup> cycles of coating performed the lowest leak current.



**Figure 5.** UV-Vis absorption spectra for TiO<sub>2</sub> thin films with different number of spin-coating

The device with the sample prepared at 3<sup>rd</sup> cycles of coating demonstrated the highest leak current. There is no increasing or decreasing trend of leak current with the number of spin coating number. For this reason, it can be concluded that the spin coating cycle does not influence the leak current.

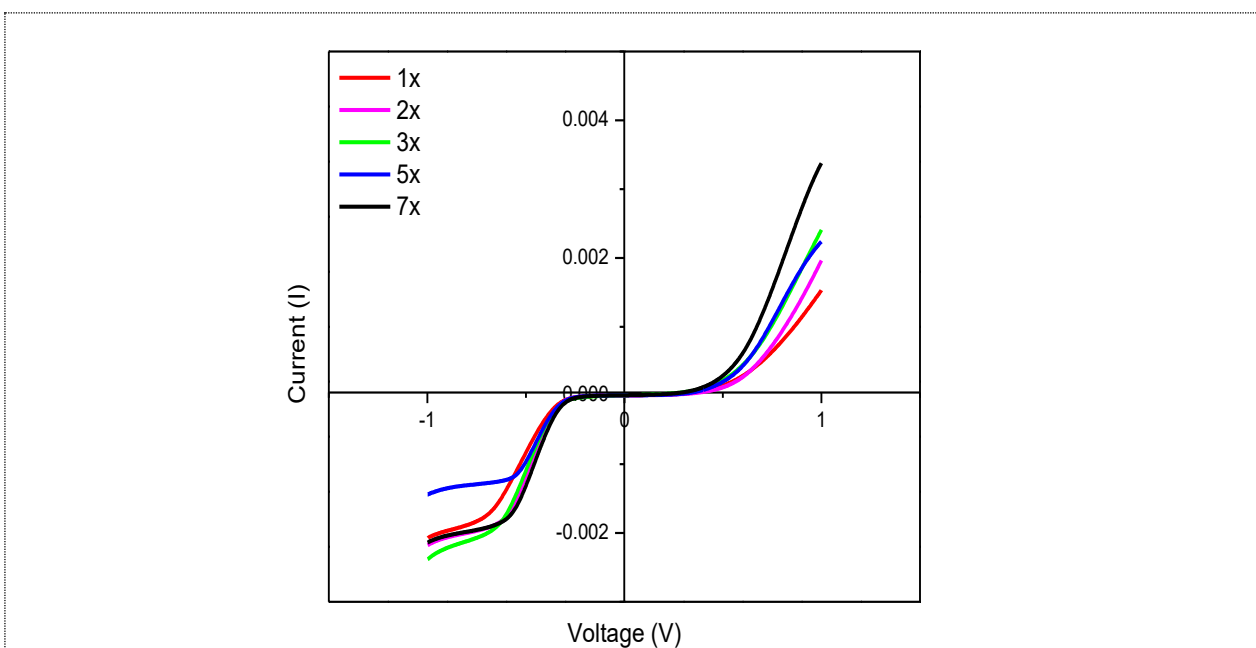


**Figure 6.** Dark current of DSSC with different TiO<sub>2</sub> spin-coating number

The comparison for  $J$ - $V$  characteristics under light illumination of the DSSC with different number of spin-coating of  $\text{TiO}_2$  thin films is shown in Fig. 7. The  $J$ - $V$  curves for all devices have high slope, causing more output power loss upon light illumination. This leads to small  $FF$  and power conversion efficiency as illustrated in Table 1. The high slope also indicates that the internal resistance in the devices is very high, leading to small photocurrent density as presented in Table 1. Also from the table, it is found that the area under  $J$ - $V$  curves increases with the number of spin coating. As discussed before, the thickness and area of optical absorption increase with the spin coating number. This indicates that higher thickness of  $\text{TiO}_2$  layer absorbs more light, which in turn generates more number of electron-hole pairs and hence enhanced the performance of the DSSC as reported by Roza et al. 2016 [13]. The photovoltaic parameters are extracted from Fig. 7 and presented in Table 1.

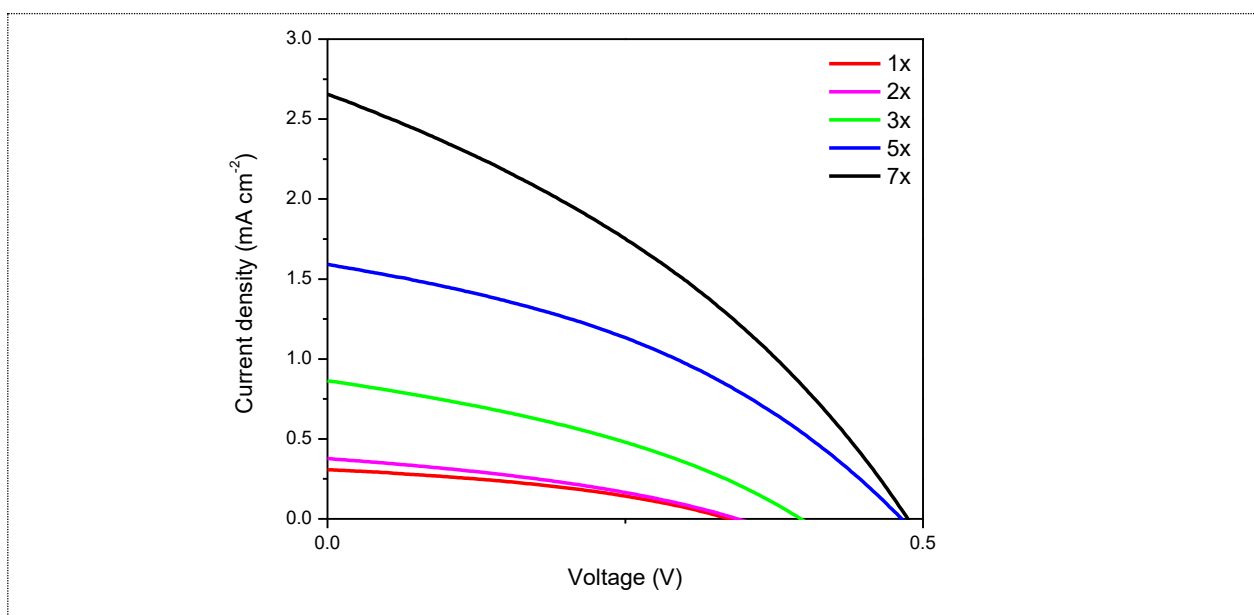


**Figure 7.**  $J$ - $V$  curves of the DSSC with different  $\text{TiO}_2$  spin-coating number under  $100 \text{ mW cm}^{-2}$  light illuminations

Fig. 8 shows the Nyquist plots of the DSSC with different  $\text{TiO}_2$  spin-coating number. The EIS data such as bulk resistance ( $R_b$ ) and charge transfer resistance ( $R_{ct}$ ) are analyzed from Fig. 8 and shown in Table 1. A straight line before semicircle represents  $R_{ct}$  and  $R_{ct}$  is presented by semi-circular curve. From Table 1, the value of  $R_b$  is the lowest when the thickness of  $\text{TiO}_2$  layer is the lowest, producing the highest  $J_{sc}$  and  $\eta$  as shown in Table 1. The  $J_{sc}$  and  $\eta$  increase as the  $R_b$  decreases and achieves the highest value at the 7<sup>th</sup> times spin-coating which are  $2.53 \text{ mA cm}^{-2}$  and 0.70%, respectively. Meanwhile, the value of  $R_{ct}$  decreases as the thickness of  $\text{TiO}_2$  films increases. This indicates that the electron transfer is faster when the thickness of  $\text{TiO}_2$  layer is higher because it provides more conducting pathways by the increase in porosity as reported by Kumari et al. 2016 [14]. The highest efficiency from this work that is 0.70% is lower than that reported by Lee et al. 2010 who fabricated the DSSC utilizing  $\text{TiO}_2$  films prepared via sol-gel technique [15]. They achieved the efficiency of 5.93% as they used longer N719 dipping time of 24 hours while ours is 15 hours. The

longer the dye dipping time, the more amount of the dye adsorbed on TiO<sub>2</sub> surface and consequently improves the amount of light absorbed by the dye. This enhances the number of electrons excited from HOMO to LUMO level of the dye to be transported to the conduction band of TiO<sub>2</sub>, hence improving the photocurrent and power conversion efficiency of DSSC.

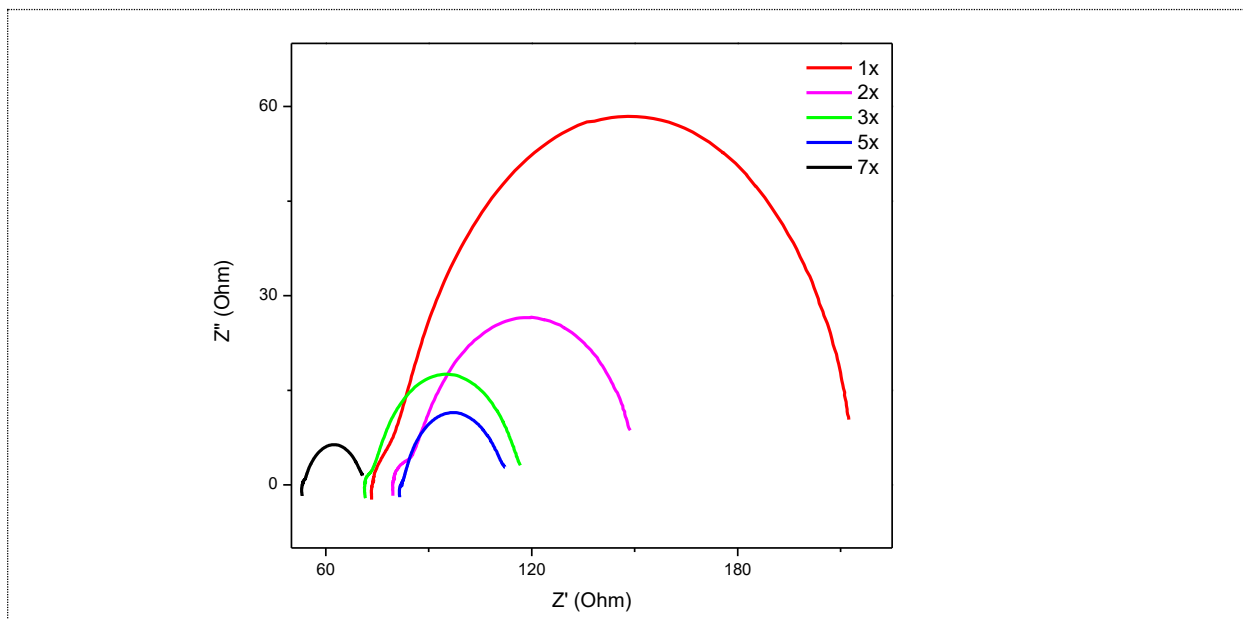


**Figure 8.** Nyquist plots of DSSC with different TiO<sub>2</sub> spin-coating number

**Table 1.** Thickness, photovoltaic parameters and EIS data for DSSC with different TiO<sub>2</sub> spin-coating number

No. of spin-coating	Thickness (nm)	$J_{sc}$ (mAcm <sup>-2</sup> )	$V_{oc}$ (V)	$FF$	$\eta$ (%)	$R_b$ ( $\Omega$ )	$R_{ct}$ ( $\Omega$ )
1	346	0.30± 0.01	0.33 ± 0.01	0.60± 0.01	0.06 ± 0.01	12.00	134.60
2	1586	0.36± 0.01	0.34 ± 0.01	0.58± 0.01	0.07± 0.01	10.00	63.60
3	2077	0.75± 0.04	0.37 ± 0.01	0.587± 0.01	0.16± 0.01	8.00	43.20
5	3841	1.52± 0.02	0.47± 0.01	0.60± 0.01	0.42± 0.01	2.00	29.20
7	5779	2.53± 0.04	0.47± 0.01	0.59± 0.01	0.70± 0.01	2.00	16.70

#### 4. CONCLUSIONS

The thickness of TiO<sub>2</sub> thin films influences the properties and performance of the DSSC device fabricated with TiO<sub>2</sub> as the photoanode which has been studied by varying the number of TiO<sub>2</sub> spin-coated on the ITO substrates. This study shows that the agglomeration of the TiO<sub>2</sub> particles reduces as the thickness of TiO<sub>2</sub> layer increases. The porosity increases with higher thickness, providing more conducting pathways for the sample to facilitate light absorption. The area of absorption window increases with spin coating number. The DSSC utilizing the sample with the highest thickness possess the highest power conversion efficiency which is 0.699 % as the device has the lowest  $R_b$  and  $R_{ct}$ .

## ACKNOWLEDGEMENTS

This work was supported by Universiti Kebangsaan Malaysia (UKM) under research grant GUP-2016-013.

## References

1. H. Shang, Y. Luo, X. Guo, X. Huang, X. Zhan, K. Jiang, Q. Meng, *Dyes and Pigments*. 87 (2010) 249-256.
2. A. Sedghi, H. N. Miankushki. *Int. J. Electrochem. Sci.* 10 (2015) 3354-3362.
3. H. Zhang, W. Wang, H. Liu, R. Wang, Y. Chen, Z. Wang, *Mater. Research B*. 49 (2014) 126-131.
4. V. Baglio, M. Girolamo, V. Antonucci, A.S. Arico. *Int. J. Electrochem. Sci.* 6 (2011) 3375-3384.
5. R. Vijayalakshmi, V. Rajendran, *Arch. Appl. Sci. Res.* 4(2) (2012) 1183-1190.
6. Y. Long, H. Xiaomei, W. Yufei, L. Jian, W. Danjun, *J Mater Sci: Mater Electron* 27 (2016) 4068-4073.
7. R. S. Sabry, Y. K. Al-Haidarie, M.A. Kudhier, *J. Sol-Gel Sci Technol.* 78 (2016) 299-306.
8. J.M. Macak, M. Zlamal, J. Krysa, P. Schmuki, *small* 2007. 3(2) (2007) 300-304.
9. M. Reinke, E. Ponomarev, Y. Kuzminykh, P. Hoffmann, *ACS Comb. Sci.* 17(7) (2015) 413-420.
10. A.B. Couto, F.L. Migliorini, M.R. Baldan, N.G. Ferreira, *ECS Transactions*. 58(30) (2014) 47-52.
11. M.M. Byranvand, A.N. Kharat, L. Fatholahu, Z.M. Beiranvand, *J. Nanostructures*. 3 (2013) 1-9.
12. A.E. Jiménez González, S. Gelover Santiago, *Semicond. Sci. Tech.* 22 (2007) 709.
13. L. Roza, M. Y. A. Rahman, A. A. Umar, M. M. Salleh, *J Mater Sci: Mater Electron*. (2016) 27:8394.
14. J.M.K.W. Kumari, N. Sanjeevadarshini, M.A.K.L. Dissayanake, G.K.R. Senadeera, C.A. Thotawatthage, *Ceylon J. Sci.* 45(1) (2016) 33-41.
15. Y. Lee, J. Chae, M. Kang, *J. Indust. Engin. Chem.* 16 (2010) 609-614.

© 2017 The Authors. Published by ESG ([www.electrochemsci.org](http://www.electrochemsci.org)). This article is an open access article distributed under the terms and conditions of the Creative Commons Attribution license (<http://creativecommons.org/licenses/by/4.0/>).